A REGIONAL SEISMIC TRAVEL TIME MODEL FOR NORTH AMERICA

Stephen C. Myers[1], Michael L. Begnaud[2], Sanford Ballard[3], Abelardo L. Ramirez[1], W. Scott Phillips[2], Michael E. Pasyanos[1], Harley Benz[4], Raymond P. Buland[4]

Lawrence Livermore National Laboratory[1], Los Alamos National Laboratory[2], Sandia National Laboratory[3], National Earthquake Information Center[4]

Sponsored by the National Nuclear Security Administration

Award Nos. DE-AC52-07NA27344[1], DE-AC52-06NA25396[2], and DE-AC04-94AL8500[3]

ABSTRACT

We extend the Regional Seismic Travel Time (RSTT) tomographic effort to North America. In previous work we developed a real-time method to capture the 1st-order effects of 3-dimensional crust and upper mantle structure on RSTTs. The model parameterization is a global tessellation of nodes with a velocity profile at each node. Interpolation of the velocity profiles generates a 3-dimensional crust and laterally variable upper mantle velocity. The upper-mantle velocity profile at each node is represented as a linear velocity gradient, which enables travel time computation in approximately 1 millisecond. Fast computation allows the model to be used in routine analyses and in operational monitoring systems. Model velocities are optimized for travel-time prediction using a tomographic formulation that adjusts the mantle velocity at the Moho, the mantle velocity gradient, and the average crustal velocity. After tomography across Eurasia, rigorous tests find that *Pn* travel time residuals are reduced from a standard deviation of approximately 1.75 seconds (ak135 model) to approximately 1.25 seconds. Further, location error is consistently reduced by approximately 45% for events located using the *Pn* phase. For North American tomography we begin by reconciling North American seismic bulletins. To these bulletins we add high-quality data sets that improve data coverage and data quality, including arrival times reported by the Array Network Facility for USArray stations. In the western United States, USArray provides unprecedented data coverage with station spacing of approximately 70 km. The National Earthquake Information Center (NEIC) researchers contribute unique ground-truth data sets that have been culled over decades. NEIC data is particularly helpful in eastern North America, where the seismicity rate is low. Arrival-time measurements from all sources are re-associated, and event locations that are best constrained by seismic data are relocated using all available arrivals. Events with known locations, e.g., explosions, are not relocated and these events help to establish absolute travel time accuracy. Seismic locations are evaluated against network coverage criteria to estimate hypocenter accuracy. The full error budget for each travel time – hypocenter uncertainty and arrival-time measurement uncertainty – is evaluated to provide a datum-specific uncertainty that establishes weighting in the tomographic inversion. Model validation includes prediction of travel times, as well as relocation of ground-truth events to measure location accuracy. Neither the travel time validation data nor the location validation data are used in the tomographic inversion.

Report Documentation Page

Form Approved
OMB No. 0704-0188

1. REPORT DATE	2. REPORT TYPE	3. DATES COVERED
SEP 2010		**00-00-2010 to 00-00-2010**

4. TITLE AND SUBTITLE	5a. CONTRACT NUMBER
A Regional Seismic Travel Time Model for North America	5b. GRANT NUMBER
	5c. PROGRAM ELEMENT NUMBER
6. AUTHOR(S)	5d. PROJECT NUMBER
	5e. TASK NUMBER
	5f. WORK UNIT NUMBER
7. PERFORMING ORGANIZATION NAME(S) AND ADDRESS(ES)	8. PERFORMING ORGANIZATION REPORT NUMBER
Los Alamos National Laboratory,P.O. Box 1663 ,Los Alamos,NM,87545	
9. SPONSORING/MONITORING AGENCY NAME(S) AND ADDRESS(ES)	10. SPONSOR/MONITOR'S ACRONYM(S)
	11. SPONSOR/MONITOR'S REPORT NUMBER(S)

12. DISTRIBUTION/AVAILABILITY STATEMENT

Approved for public release; distribution unlimited

13. SUPPLEMENTARY NOTES

Published in Proceedings of the 2010 Monitoring Research Review - Ground-Based Nuclear Explosion Monitoring Technologies, 21-23 September 2010, Orlando, FL. Volume I. Sponsored by the Air Force Research Laboratory (AFRL) and the National Nuclear Security Administration (NNSA). U.S. Government or Federal Rights License

14. ABSTRACT

We extend the Regional Seismic Travel Time (RSTT) tomographic effort to North America. In previous work we developed a real-time method to capture the 1st-order effects of 3-dimensional crust and upper mantle structure on RSTTs. The model parameterization is a global tessellation of nodes with a velocity profile at each node. Interpolation of the velocity profiles generates a 3-dimensional crust and laterally variable upper mantle velocity. The upper-mantle velocity profile at each node is represented as a linear velocity gradient, which enables travel time computation in approximately 1 millisecond. Fast computation allows the model to be used in routine analyses and in operational monitoring systems. Model velocities are optimized for travel-time prediction using a tomographic formulation that adjusts the mantle velocity at the Moho, the mantle velocity gradient, and the average crustal velocity. After tomography across Eurasia rigorous tests find that Pn travel time residuals are reduced from a standard deviation of approximately 1.75 seconds (ak135 model) to approximately 1.25 seconds. Further, location error is consistently reduced by approximately 45% for events located using the Pn phase. For North American tomography we begin by reconciling North American seismic bulletins. To these bulletins we add high-quality data sets that improve data coverage and data quality, including arrival times reported by the Array Network Facility for USArray stations. In the western United States, USArray provides unprecedented data coverage with station spacing of approximately 70 km. The National Earthquake Information Center (NEIC) researchers contribute unique ground-truth data sets that have been culled over decades. NEIC data is particularly helpful in eastern North America, where the seismicity rate is low. Arrival-time measurements from all sources are re-associated, and event locations that are best constrained by seismic data are relocated using all available arrivals. Events with known locations, e.g., explosions, are not relocated and these events help to establish absolute travel time accuracy. Seismic locations are evaluated against network coverage criteria to estimate hypocenter accuracy. The full error budget for each travel time ? hypocenter uncertainty and arrival-time measurement uncertainty ? is evaluated to provide a datum-specific uncertainty that establishes weighting in the tomographic inversion. Model validation includes prediction of travel times, as well as relocation of ground-truth events to measure location accuracy. Neither the travel time validation data nor the location validation data are used in the tomographic inversion.

15. SUBJECT TERMS

16. SECURITY CLASSIFICATION OF:			17. LIMITATION OF ABSTRACT	18. NUMBER OF PAGES	19a. NAME OF RESPONSIBLE PERSON
a. REPORT	b. ABSTRACT	c. THIS PAGE			
unclassified	**unclassified**	**unclassified**	**Same as Report (SAR)**	**10**	

OBJECTIVES

Monitoring seismic events at ever-lower magnitude thresholds requires the utilization of seismic stations that are close to the event. The proliferation of seismic stations across the globe results in lower seismic detection thresholds because more stations are likely to be at regional distance to an event. However, utilization of arrival time data at regional distances often results in degraded location accuracy, because large variations in regional crust and upper-mantle structure can result in large travel time prediction errors.

In previous work we successfully developed an operations-oriented method to account for the 1st-order effects of 3-dimensional crust and upper mantle structure on RSTTs (Myers et al., 2010). The RSTT model parameterization is a global tessellation of nodes, so any model in RSTT format is inherently global in extent and a regional travel time can be computed anywhere for the dominant regional phases (*Pn*, *Pg*, *Sn*, and *Lg*). However, in order to improve travel time prediction accuracy over conventional methods, the model must be "tuned" along each ray path. RSTT model tuning is accomplished by first constructing a best approximation to the 3-dimensional structure of the Earth's crust and upper-most mantle based on existing models. Model velocity – but not layer interfaces – are then adjusted using tomographic imaging methods to further improve prediction accuracy. RSTT model refinement was conducted first over the ~1/4 of the globe containing Eurasia and North Africa (Myers et al., 2010; Figure 1). RSTT tomography across Eurasia and North Africa results in a factor ~2 improvement in location accuracy.

Here we extend RSTT tomography to North America. By extending tomography to North America we address the need to improve global tomographic coverage, which is desirable for CTBT monitoring, and we motivate RSTT use at the NEIC, whose primary interest is monitoring earthquakes in the continental U.S.

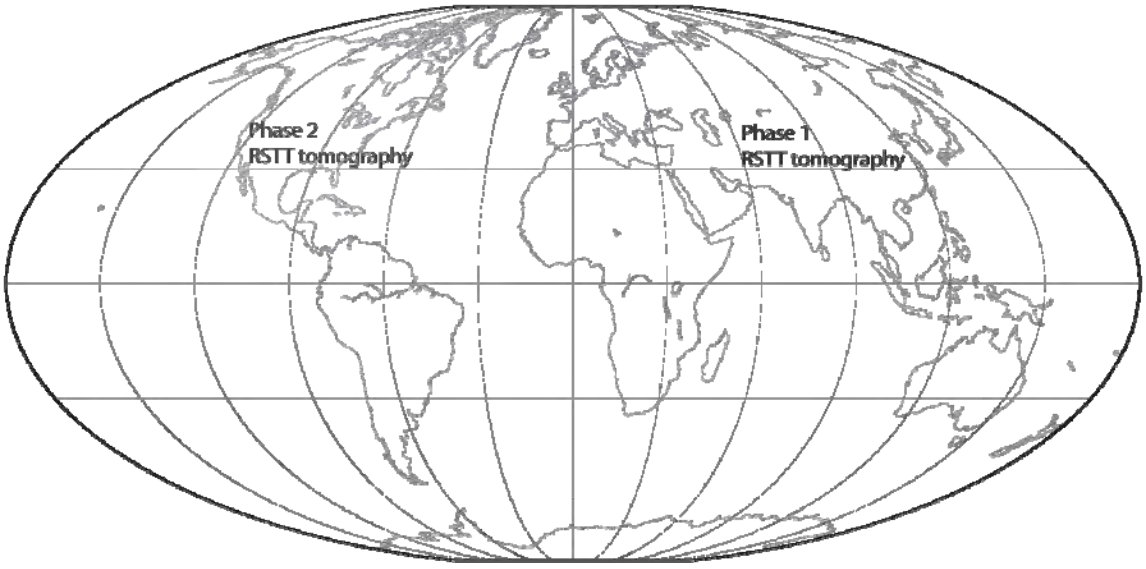

Figure 1. Phased approach for applying RSTT tomography, with the end goal of producing a global model for the universal prediction of regional phases. Phase 1 is complete, and Phase 2 would be initiated under this proposal. (Reproduced from Myers et al., 2010)

RESEARCH ACCOMPLISHED

Work Plan

RSTT model refinement has 5 essential components. First, based on previously determined models, a prior model is built that includes lateral variability of the geologic layers that comprise the crust. The prior model also includes lateral variability of *P*-wave and *S*-wave velocity in the crustal layers and in the upper mantle. A good prior model is essential because the RSTT tomography inversion is invariably under determined, necessitating a model search in the neighborhood of the starting model. Second, a high-quality data set of event locations and arrival-time observations is compiled for use in tomography and for model validation. Third, tomographic inversion is used to adjust model velocities so that travel time predictions are in agreement with the high-quality data set. Layer boundaries are not adjusted in the tomographic inversion because RSTT data sets cannot adequately resolve the trade-off between boundary depth and velocity. Fourth, assessment of travel time error is accomplished by comparing model predictions to the validation data set (not used in tomography). The fifth step is model validation, in which events with known locations are relocated to measure location accuracy and compare observed location error with estimates derived from model uncertainty.

To date, we have completed the data compilation effort, begun evaluation of the CRUST2.0 starting model, and conducted preliminary tomographic inversions. We report on the data set and on our preliminary findings.

Model Parameterization

Myers et al. (2010) provide a detailed description of RSTT model parameterization, travel time calculation, and tomographic formulation, and we provide a brief review here. Crust and upper mantle velocity structure are represented using radial velocity profiles at geographically distributed nodes (Figure 2). The nodes form a triangular tessellation that seamlessly covers the globe. Node spacing is approximately 1° for the model presented here. Node spacing may be adjusted as needed, and we plan to investigate the use of 0.25° node spacing in North America that may be warranted by outstanding data coverage in the western U.S. Velocity interfaces are defined by the radial distance from the center of the Earth, which allows us to explicitly build the GRS80 ellipsoid (Moritz, 1980) into the model and obviate travel-time corrections for ellipticity.

We adopt the velocity versus depth profile in the crust from Pasyanos et al. (2004), which includes model layers for water, 3 types of sediments, upper crystalline crust, middle crust, and lower crust (Figure 2). The crustal layers overlay a mantle velocity profile that is simplified to two parameters: velocity at the Moho and a linear velocity gradient with depth. By interpolating model parameters from surrounding nodes – layer thickness, velocity, and mantle gradient – we generate a continuous model of the 3-D crust and laterally varying upper mantle.

Travel Time Calculation

Parameterization of upper mantle velocity with a linear gradient facilitates an approximation for *Pn* travel time that enables real-time computation (~1 millisecond). Computation of *Pn* travel time at near-regional distance (<700 km) commonly assumes that the *Pn* phase propagates as a head wave, with a ray-path that follows the contour of the Moho (e.g. Hearn, 1984). The head wave assumption results in poor travel time prediction at far-regional distance (>~700 km) because the *Pn* ray can dive appreciably into the mantle due to a positive velocity gradient with depth and Earth sphericity (e.g,. Zhao and Xie, 1993; Ritzwoller et al., 2003; Hearn et al., 2004). To more accurately predict *Pn* at far-regional distances, Zhao (1993) and Zhao and Xie (1993) employ a constant linear velocity gradient in the upper mantle for the whole study area.

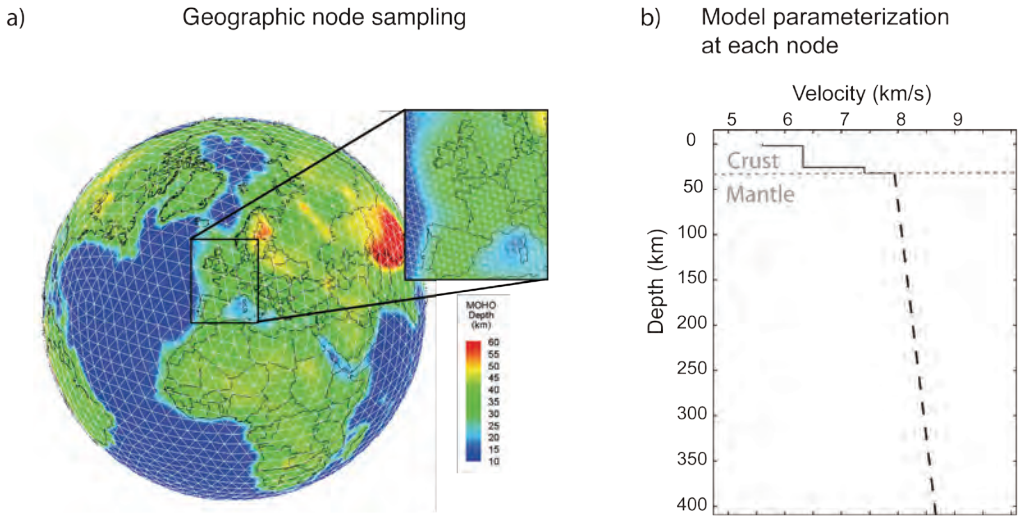

Figure 2. Global model parameterization. a) An example tessellation with approximately 5° grid spacing. The inset shows the 1° used in this study. Color indicates Moho depth of the starting model. b) An example velocity/depth profile as defined at each node. The mantle portion of the profile is specified by the velocity at the crust/mantle interface and a linear gradient. (Reproduced from Myers et al., 2010)

The Zhao (1993) and Zhao and Xie (1993) travel-time calculation is similar to the widely used approach of Hearn (1984), with an additional term (γ) introduced to account for diving rays. The travel-time calculation is

$$TT = \sum_{i=1}^{N} d_i s_i + \alpha + \beta + \gamma \qquad (1)$$

where *d* and *s* are the distance and slowness (taken as 1/velocity below the Moho) in each of the *i* segments comprising the great-circle path between Moho pierce points near the event and station, α and β are the crustal travel times at the source and receiver, and γ (described below).

From Zhao (1993) and Zhao and Xie (1993),

$$\gamma = \frac{c^2 X_m^3}{24 V_0} \qquad (2)$$

where X_m is the horizontal distance traveled in the mantle, and V_0 is a regional average of mantle velocity at the Moho. $c = g * s + 1/r$, where 1/r is an Earth flattening correction and r is the radius at which a ray enters and exits the linear velocity gradient, g (Helmberger, 1973; Zhao and Xie, 1993). This approximation is valid when $ch << 1$, where h is the bottoming depth of the ray in a linear velocity gradient.

We use a spatially varying mantle velocity gradient, *c* (Phillips et al., 2007), and we calculate γ by averaging *c* along the ray track. V_0 remains an average *Pn* velocity over the whole model, which allows us to take advantage of linear tomographic inversion methods (see below). Tests find that using a global average for V_0 introduces negligible travel-time error when *Pn* velocities range from 7.5 km/s to 8.3 km/s.

Data

Ongoing GNEM R&D integration efforts include the collection of seismic bulletins that comprise the vast majority of events and arrival time measurements that are available in North America. To these ongoing efforts we add additional high-quality data sets that provide coverage in specific areas. The USarray project (http://www.iris.edu/USArray/researchers/data.html) is providing unprecedented coverage with station spacing of approximately 70 km. The transportable USarray is a staged deployment that began on the west coast of the U.S. and is steadily moving eastward. USarray currently straddles the Rocky Mountain front

and the Great Plains. The transportable array is scheduled to reach the Eastern US in 2013. Because of the dense station spacing, arrival time measurements of regional distance events at USArray stations can constrain short wavelength lateral variations in the crust and upper mantle. We have loaded the arrival time measurements from the Array Network Facility (http://anf.ucsd.edu) into the GNEM R&D database and reconcile the events/arrivals with existing holdings. Second, NEIC researchers have collected unique ground truth data sets in North America, particularly in the Eastern U.S. The NEIC data have been integrated/reconciled with GNEM R&D holdings in a similar fashion as the ANF data.

Data processing follows the procedure outlined in Myers et al. (2010). Epicenter accuracy for each event in the reconciled bulletin is assessed using the network coverage criteria of Bondár et al. (2004). We further add non-seismic constraints based on known explosion locations, ground displacement from interferometric synthetic aperture radar (InSAR), and mine locations. To diminish the possibility of introducing travel times for phases that interact with velocity discontinuities at ~410 km and ~660 km, the maximum event-station distance range is set to 15°. The minimum event-station distance range is determined by the post-critical refraction for a wave interacting with the Moho. In practice, the minimum distance varies from tens of km in the ocean (thin crust) to approximately 200 km in regions of thick crust.

Because the goal of this work is to produce a model for *Pn* travel-time prediction for real-time monitoring, it is important that *Pn* prediction error is unbiased relative to teleseismic *P*-wave prediction error. Previous efforts have achieved unbiased *Pn* error by using an *ad hoc* travel time correction (Yang et al., 2004). To achieve unbiased *Pn* error, we recomputed each event origin time using at least 10 *P*-wave arrivals. The hypocenter is then fixed during the tomographic procedure, which forces *Pn* prediction error to be unbiased relative to teleseismic P-wave error.

All picks are evaluated against an uncertainty budget that accounts for event mislocation, a global average of *ak135* prediction uncertainty, and arrival-time measurement uncertainty (See Myers et al., 2010). Following removal of local outliers, we produce summary rays for each station by averaging residuals for events that are within 0.25° of one another (Figure 3).

For North America we begin with 80728 *Pn* paths. Outlier removal reduces the number of paths to 70514, of which 7575 are set aside for validation. Use of summary rays reduces the number of paths from 62939 to 35736. The standard deviation of the initial *Pn* data set (80728 paths) is 2.71 seconds with a mean of 0.81 seconds. After outlier remove the standard deviation is reduced to 2.35 seconds with a mean of 0.78 seconds.

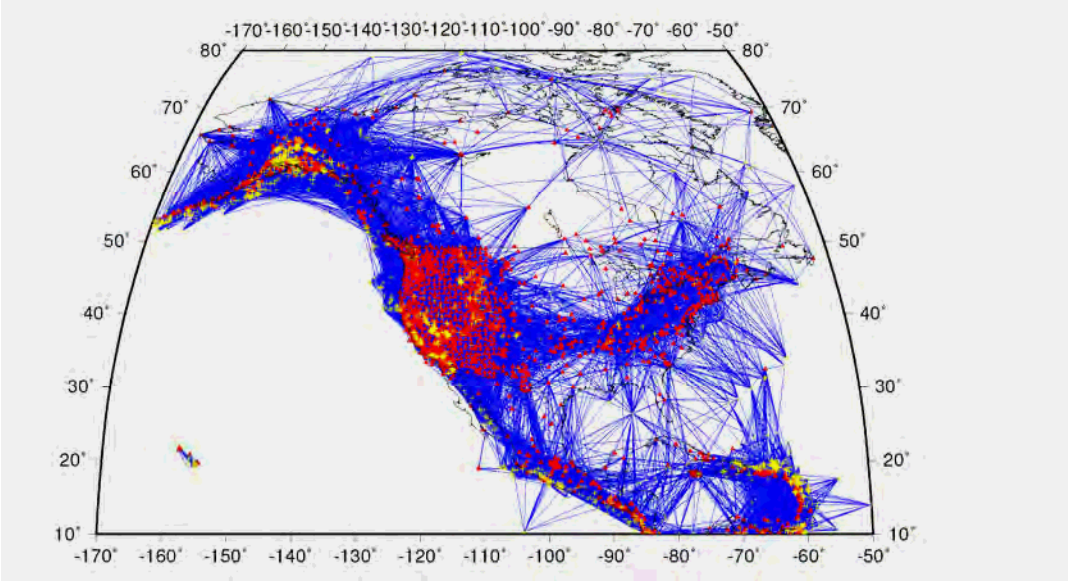

Figure 3. RSTT *Pn* summary ray paths for North America. Stations are red triangles and events are yellow "pluses".

Tomography

The *Pn* travel time (Equation 1) lends itself to a linear tomographic formulation. Because our primary objective is to improve travel-time prediction, we avoid the use of parameters that would not be part of a subsequent travel-time calculation (e.g. event and station time terms). In matrix form, the tomographic system of equations is:

$$\begin{bmatrix} x_1^1 & \cdots & x_N^1 & -\frac{x_1^1 (X_m)^3}{24 V_o X_m} & \cdots & -\frac{x_N^1 (X_m)^3}{24 V_o X_m} & \sum_{p=1}^{Q} \frac{l_{1p}^1}{v_{1p}} & \cdots & \sum_{p=1}^{Q} \frac{l_{Np}^1}{v_{Np}} \\ \vdots & & & & \ddots & & & & \vdots \\ x_1^K & \cdots & x_N^K & -\frac{x_1^K (X_m)^3}{24 V_o X_m} & \cdots & -\frac{x_N^K (X_m)^3}{24 V_o X_m} & \sum_{p=1}^{Q} \frac{l_{1p}^K}{v_{1p}} & \cdots & \sum_{p=1}^{Q} \frac{l_{Np}^K}{v_{Np}} \\ & & & & & \text{Regularization} & & & \end{bmatrix} * \begin{bmatrix} s_1 \\ \vdots \\ s_N \\ c_1^2 \\ \vdots \\ c_N^2 \\ a_1 \\ \vdots \\ a_N \end{bmatrix} = \begin{bmatrix} t^1 \\ \vdots \\ t^K \\ \text{Regularization} \end{bmatrix} \quad (3)$$

where

t = *travel time*
s = *mantle slowness below the Moho (a.k.a. Pn slowness)*
x = *Pn distance (or weight) for each model node*
c = *normalized velocity gradient, v=vo(1+cz)*
X_m = *length of Pn ray path in the mantle*
Vo = *average Pn velocity*
v = *velocity of a crustal layer*
k = *index on K paths (travel-time observations)*
p = *index on Q crustal layers*
l = *length of the ray path in a specified crustal layer (determined by layer thickness and ray parameter in Equations (2) and (3)).*
a = *node-specific adjustment to the slowness of each crustal layer (crustal modifier).*

The tomographic equation solves for the model slowness below the Moho, *s* (a.k.a. *Pn* slowness), the square of mantle velocity gradient, c^2, and a scalar adjustment to crustal slowness, *a*. The formulation in Equation 3 is similar to the approach presented in Phillips et al. (2007), with the difference that we use a scalar adjustment to the slowness of the crustal stack, as opposed to a time term, to account for travel-time errors in crustal legs of the *Pn* ray. The crustal legs can impart as much or more error on the travel time prediction as the travel time in the mantle. Because our goal is to accurately predict subsequent travel times using the tomographic model, it is important to fold all adjustments affecting travel time into the model, rather than absorb the error in a time term that is discarded and will not be used in subsequent travel time prediction.

Preliminary Results

Initial tomgraphic inversions for North America are consistent with the broad trends in previous studies (Figures 4, 5, and 6). The mantle velocity at the Moho approaches 8.3 km/s across much of the Canadian Shield and drops to between 8.0 km/s and 8.15 km/s in the Eastern U.S. (Figure 4). West of the Rocky Mountain Front, velocity drops abruptly below 8 km/s, with low-velocity anomalies of approximately 7.7 km/s in some places.

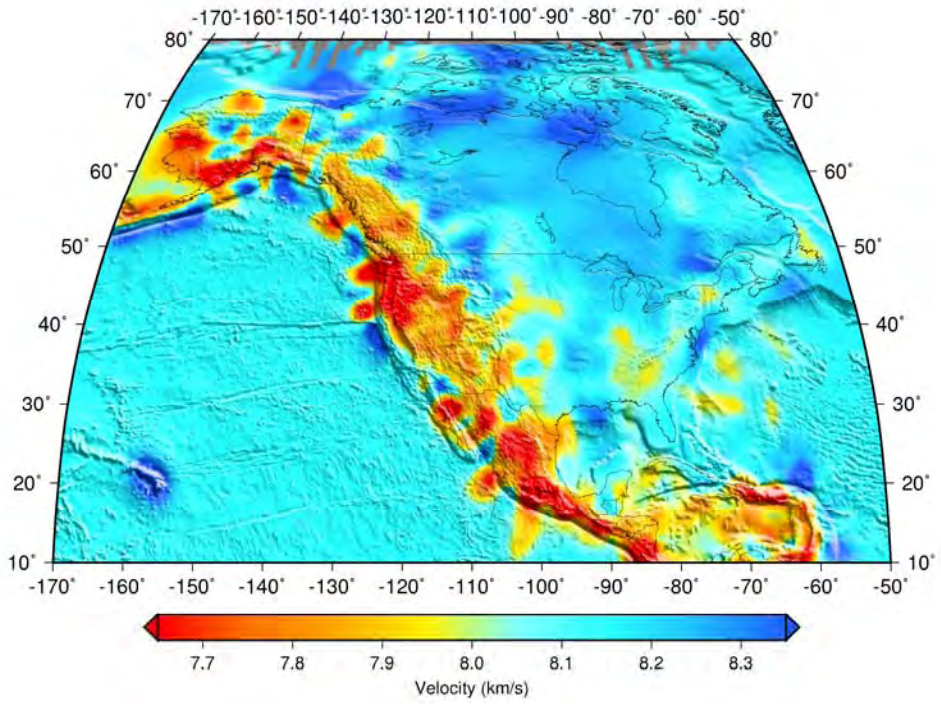

Figure 4. Mantle velocity at the Moho. RSTT tomography is consistent with the known pattern of upper-mantle velocity: very fast across the Canadian Shield; fast across the eastern U.S., and slow west of the Rocky Mountain Front.

The pattern of velocity gradient in the mantle is dominated by oceanic subduction (Figure 5). Subduction of high velocity oceanic lithosphere creates complex three-dimensional structure that cannot be fully captured by the RSTT model parameterization. However, the first-order effect on *Pn* travel times is early arrival at far-regional distances when rays dive into the mantle and preferentially channel through the high-velocity ocean lithosphere. RSTT captures this travel-time effect with a strong velocity gradient, as seen in southern Alaska, the Pacific Northwest, southern Mexico, and the Caribbean. Other areas of high gradient include the Wyoming Archean terrain and the central U.S. We expect the Canadian Shield have a strong velocity gradient, but the tomographic data set, which only has a few long paths across the Canadian Shield, is not suited to resolve mantle gradient in the Canadian Shield. In subsequent inversions we may force a high gradient in the Canadian Shield.

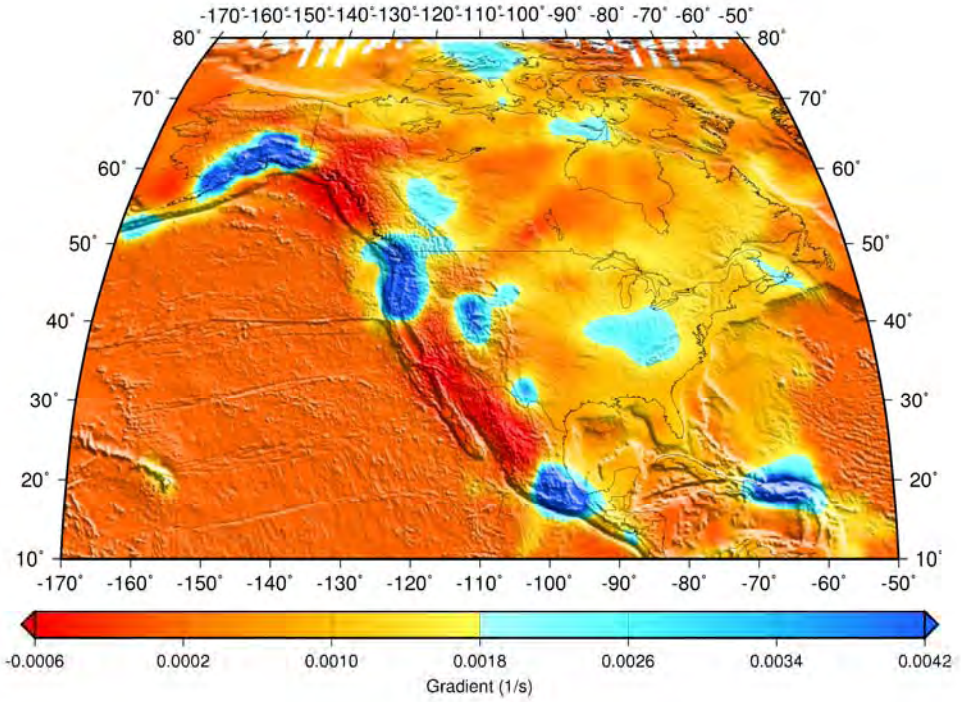

Figure 5. Mantle velocity gradient. Subduction zones are characterized with a high velocity gradient.

Figure 6 shows the modification to crustal slowness (*a* in equation 3). The *Pn* data set does not provide resolution of each of the 7 layers that comprise the RSTT crust, so we solve for a single modification to crustal slowness at each node that is uniformly applied each crustal layer. Increases in crustal velocity (negative *a* values) are seen in California and Idaho. Decreases in crustal velocity are seen in the Colorado Plateau, Wyoming, and the Wrangle Mountains of Alaska. The crustal velocity does not change significantly throughout eastern North America.

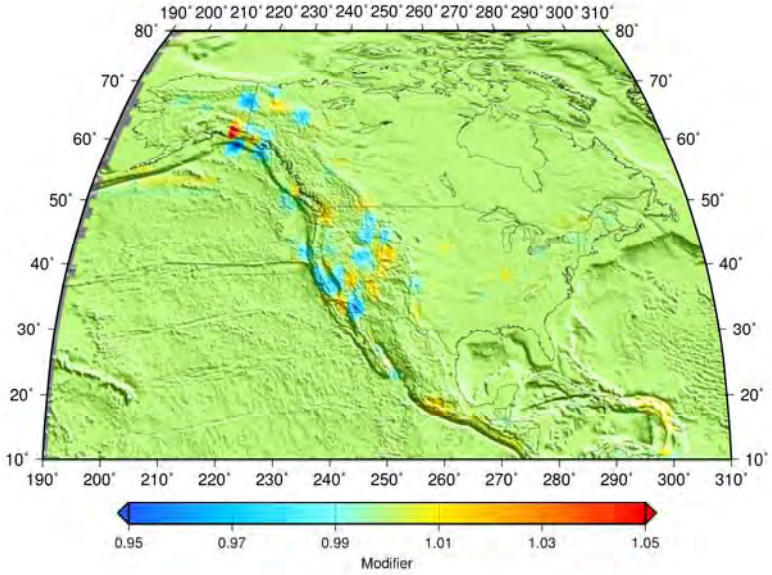

Figure 6. Modification of crustal slowness. This term adjusts the slowness (1/velocity) of the whole crustal stack.

Validation

We leave out 10% of the tomographic data for use in non-circular validation tests. The validation data provides sampling across North America, so residual summary statistics are a good measure of expected model performance in monitoring systems. Figure 7 shows travel time error as a function of distance for the *ak135* model, and the RSTT model. In this case error is represented as the average residual in successive distance bins. Similar to the Eurasia results, *ak135* uncertainty is approximately 2 seconds at near-regional distance and increases rapidly beyond 5° to a maximum of almost 3 seconds at far-regional distance. The RSTT model is significantly improved over *ak135* by reducing the overall travel time prediction error down to approximately 1.5 seconds. The trend of increasing residuals as a function of distance is still evident in the preliminary model.

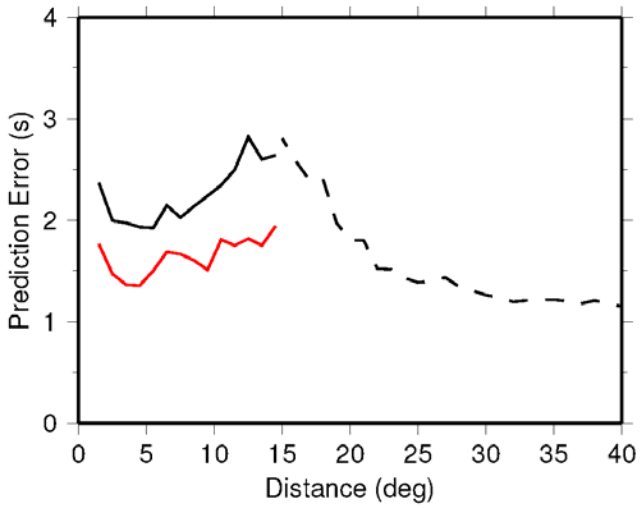

Figure 7. *Pn* travel time prediction error as a function of distance for North American validation data set: black line is ak135, red line is RSTT.

CONCLUSIONS AND RECOMMENDATIONS

We have completed the data compilation needed to extend RSTT tomography to North America. That effort includes integration into our database of data provided by the NEIC and picks provided by the Array Network Facility for USArray stations. The integrated data have been relocated and epicenter accuracy criteria applied. Pick outliers have been identified based on overall statistics and comparison with neighboring data. Summary rays for the Pn data (Figure 3) provide excellent ray coverage across western North America, good coverage across the eastern U.S., poor coverage across central and eastern Canada.

Preliminary tomographic results use a starting model that is based on CRUST2.0. We find that modification to CRUST2.0 are needed. Nonetheless, preliminary tomographic results are consistent with known velocities for major tectonic provinces. Tests of travel-time prediction based on a validation data set (Figure7) show approximately 25% reduction in the standard deviation of residuals.

ACKNOWLEDGEMENTS

We thank our colleagues and collaborators at AFTAC, who worked closely with us at the formative stages of the RSTT project.

REFERENCES

Bondár, I., S. C. Myers, E. R. Engdahl, and E. A. Bergman (2004). Epicenter accuracy based on seismic network criteria, *Geophys. Jour. Int*., 156**,** 483–496.

Bondár, I., K. L. McLaughlin (2009). A New Ground Truth Data Set For Seismic Studies, *Seismol. Res. Lett*. 80: 3.

Hearn, T. M. (1984). Pn travel times in southern California, *Jour. Geophys. Res*. 89: 1843–1855.

Hearn, T. M., S. Wang, J. F. Ni, Z. Xu, Y. Yu, and X. Zhang (2004). Uppermost mantle velocities beneath China and surrounding regions, *J. Geophys. Res*. 109: B11301, doi:10.1029/2003JB002874.

Helmberger, D. V. (1973). Numerical seismograms of long-period body waves from seventeen to forty degrees, *Bull. Seismol. Soc. Am*. 63: 633–646.

Hestenes, M. R., and E. Stiefel (1952). Methods of conjugate gradients for solving linear systems, *J. Res. Nat. Bur. Stand*., 49 (6).

Johnson, M., and C. Vincent (2002). Development and testing of a 3-D velocity model for improved event location: A case study for the India-Pakistan region, *Bull. Seismol. Soc. Am*. 92: 2893–2910.

Kennett, B. J. N., E. R. Engdahl and R. Buland (1995). Constraints on seismic velocities in the Earth from traveltimes, *Geophys. J. Int*, 122: 108–124.

Moritz, H. (1980). Geodetic reference system 1980. Bull. Geodesique. Paris, 54 (3).

Myers, S.C., M. L. Begnaud, S. Ballard, M. E. Pasyanos, W. S. Phillips, A. L. Ramirez, M. S. Antolik, K. D. Hutchenson, J. Dwyer, and C. A. Rowe, and G. S. Wagner (2009). A crust and upper mantle model of Eurasia and North Africa for Pn travel time calculation, *Bull. Seismol. Soc. Am*. 100: 640–656.

Pasyanos, M. E., W. R. Walter, M. P. Flanagan, P. Goldstein, and J. Bhattacharyya (2004). Building and testing an a priori geophysical model for western Eurasia and North Africa, *Pure. Appl. Geophys*. 161: 235–281.

Phillips, W. S., M. L. Begnaud, C. A. Rowe, L. K. Steck, S. C. Myers, M. E. Pasyanos, and S. Ballard (2007). Accounting for lateral variations of the upper mantle gradient in Pn tomography studies, *Geophys. Res. Lett*. 34: doi:10.1029/2007GL029338, 2007.

Steck, L. K., C. A. Rowe, M. L. Begnaud, W. S. Phillips, V. L. Gee, and A. A. Velasco (2004), Advancing seismic event location through difference constraints and three-dimensional models, in *Proceedings of the 26th Seismic Research Review - Trends in Nuclear Explosion Monitoring*, LA-UR-04-5801, Vol. 1, pp. 346–355.

Yang, X., I. Bondár, J. Bhattacharyya, M. Ritzwoller, N. Shapiro, M. Antolik, G. Ekstro¨m, H. Israelsson, and K. McLaughlin (2004). Validation of Regional and Teleseismic Travel-Time Models by Relocating Ground-Truth Events, *Bull. Seismol. Soc. Am*. 94: 897–919.

Zhao, L.-S. (1993). Lateral variations and azimuthal isotropy of *Pn* velocities beneath Basin and Range province, *J. Geophys. Res*. 98: 22,109–22,122.

Zhao, L.-S., and J. Xie (1993). Lateral variations in compressional velocities beneath the Tibetan Plateau from Pn traveltime tomography, *Geophys. J. Int*. 115: 1070–1084.